2021-03

The characteristics of atmospheric particles and metal elements during winter in Beijing: Size distribution, source analysis, and environmental risk assessment

Zhi, M

10.1016/j.ecoenv.2021.111937
Ecotoxicology and Environmental Safety
Elsevier BV

The characteristics of atmospheric particles and metal elements during winter in Beijing: size distribution, source analysis, and environmental risk assessment

Minkang Zhi [a], Xi Zhang [b], Kai Zhang [a]*, Simon J. Ussher [c], Wenli Lv [a], Yuqian Luo [a]

[a] State Key Laboratory of Environmental Standards and Risk Assessment, Chinese Research Academy of Environmental Sciences, Beijing 100012, China

[b] Faculty of Environmental Engineering, The University of Kitakyushu, 1-1 Hibikino, Wakamatsu, Kitakyushu, Fukuoka 808-0135, Japan

[c] School of Geography, Earth and Environmental Sciences, University of Plymouth, Plymouth PL4 8AA, United Kingdom

Abstract: In order to investigate the pollution characteristics of size-segregated particles and metal elements (MEs) after the *Chinese Air Pollution Prevention Action Plan* was released in 2013, an intensive field campaign was conducted in the suburban area of Chaoyang District, Beijing in winter 2016. The size distributions of particle mass concentrations were bimodal, with the first peak in the fine fraction (0.4~2.1 μm) and the second peak in the coarse fraction (3.3~5.8 μm). Moreover, the proportion of fine particles increased and the proportion of coarse particles decreased as the pollution level was more elevated. It was found that the composition of coarse particles is as important as that of fine particles when pollution of aerosol metals in the atmosphere in 2016 were compared to 2013. In addition, according to the size distribution characteristics, 23 MEs were divided into three groups: (a) Fe, Co, Sr, Al, Ti, Ba, and U, which concentrated in coarse mode; (b) Zn, As, Cd, Tl, and Pb, which concentrated in fine mode; and (c) Na, K, Be, V, Cr, Mn, Ni, Cu, Mo, Ag, and Sn, showing bimodal distribution. Under clean air, slight pollution and moderate pollution conditions, most elements maintained their original size distributions, while under severe pollution, the unimodal distributions of most MEs became bimodal distributions. The factors analysis combined with size distributions indicated that Na, Zn, Mo, Ag, Cd, and Tl, showing the moderate to severe contamination on environment, were significantly influenced by diffuse regional emissions or anthropogenic source emissions (vehicle exhaust emissions and combustion process). The environmental risk assessment revealed that the heavy metal loading in the atmospheric particles collected had a high potential for

ecological risk to the environment during sampling period because of the high contribution of Cd, Tl, Zn and Pb.

Key words: **trace** metals; heavy metals; size distribution; aerosol; Enrichment factor; Ecological risk; particulate matter

1. Introduction

In recent years, pollution of metal elements (MEs) in atmospheric particles has aroused great attention because of its adverse effect on the environment (Schwartz et al., 1996; Zhai et al., 2019). Airborne MEs account for a minor proportion of atmospheric aerosols by mass (Bilos et al., 2001; Karaca et al., 2009; Liu et al., 2013; Pancras et al., 2013), but contribute significantly to overall air pollution due to the toxicity of MEs, particularly heavy metal elements, which are also non-degradable and bio-enriched (Kampa and Castanas, 2008; Pacyna and Pacyna, 2001). These MEs can break the balance of atmospheric environment to a large extent (Gregory et al., 1996). MEs deposited to the Earth's surface also affect the aquatic and soil ecosystem (Wei et al., 2019; Woszczyk et al., 2018). In addition, these effects on the ecology and environment not only strongly depend on the concentrations and physico-chemical properties of MEs, but also have a close association with their size distributions in particles (Eleftheriadis et al., 2014; Taner et al., 2013; Yu and Huang, 2008). Some previous research has shown that PM_{10} exists in the local atmosphere and settles into soil, plants and water through wet and dry deposition, which has an impact on local ecosystem, whereas $PM_{2.5}$ can exert the influence on regional ecosystem by transporting far from emission sources (Hao et al., 2018; Kampa and Castanas, 2008). And MEs are distributed among the wide aerodynamic size range of their constituent particles (Polidori et al., 2009). Thus, the combination of concentrations and size distributions of MEs is significant to assess the ecological risk assessment qualitatively and quantitatively. Moreover, detailed information on the size distribution of MEs is essential to identify their sources (Gao et al., 2016; Pan et al., 2015).

Many previous studies have investigated the size distribution of MEs in different function areas (Allen et al., 2001; Silva et al., 1999; Zereini et al., 2005). The elemental

content of atmospheric particles is closely related to their size distribution, which is directly influenced by the origin of the emissions from natural and anthropogenic sources (Acosta et al., 2011; Lee et al., 2013). Li et al. (2012) found that the relatively high concentrations of heavy metals were generally loaded on fine particles. Duan et al. (2014) draw the conclusion that the ratios of atmospheric heavy metals such as Pb, Cd, Zn, As, Cu, Cr, Ni, Mn, and V in fine particles to those in inhalable particles were from 46.8% to 88.5%, in accord with the research of Tan et al. (2017) and Wang et al. (2013). As a result of rapid urbanization, Beijing has been a hotspot subject to anthropogenic emissions of MEs (Tian et al., 2012), particularly during the heating period in autumn and winter. However, the *Chinese Air Pollution Prevention Action Plan* was released in 2013, resulting in the removal of many sites of heavy-polluting industriesfrom Beijing.This has already shown to have had positive effects on the atmospheric pollution situation (Wang et al., 2010). Hence, it is essential to analyze the size distributions of atmospheric particles and MEs in Beijing under the new pollution background.

This study presented the characteristics of 23 MEs in size-resolved aerosols collected from an intensive field campaign in Beijing in winter 2016, during which the air quality was highly variable. The objectives of the research were (1) to investigate the size distributions of atmospheric particles and selected 23 MEs under different air quality levels, (2) to identify the sources of MEs, and (3) to evaluate the environmental risks of heavy metals.

2. Materials and methods

2.1 Sampling

The sampling campaign of atmospheric particle collection was carried out at the Chinese Research Academy of Environment Science (CRAES，40.03°N、116.39°E) (Fig. 1). The site is located outside the 5th ring road in a suburban area of Chaoyang District, Beijing with a height of 10 m. It is a mixed commercial and residential area and is influenced by traffic emission, to the west is an arterial road, with a west-east secondary trunk road of 100m in the south and residential buildings on both sides.

Otherwise, there are no other obvious nearby sources of pollution.

The size-resolved atmospheric particles were collected using an ambient 8-stage cascade impactor sampler (Anderson Series 20-800, BGI-TISCH Inc., USA) with cut-offs of 9.0, 5.8, 4.7, 3.3, 2.1, 1.1, 0.7, and 0.4 μm, operating at a flow rate of 28.3 L·min $^{-1}$ in this experiment. The particle size ranges corresponding to the level of the sampler and human organ in the respiratory system where the different size particles can be deposited was summarized in Table 1. The sampling period was from January to March 2016. Each sampling lasted 48h and conducted every three times per month (the first, middle and late ten days of every month). Finally, a total of 8 groups of samples were obtained.

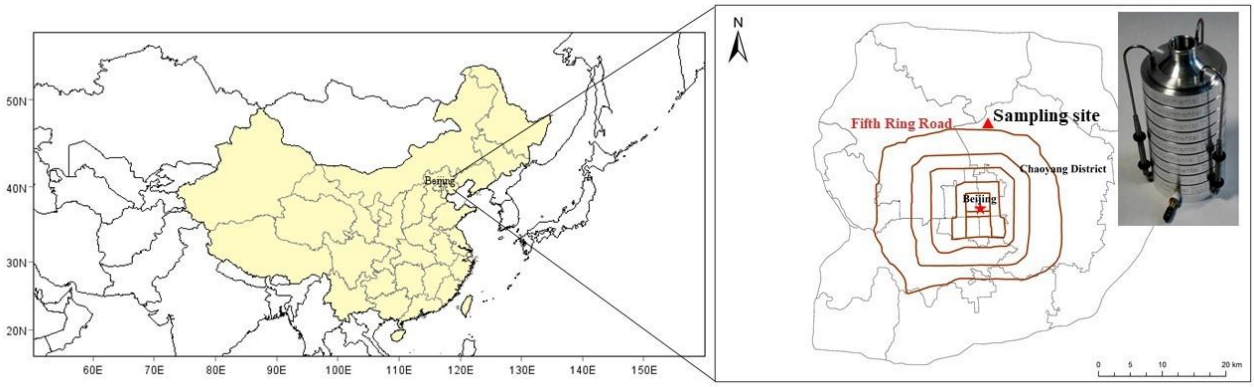

Fig. 1. The location of sampling site

Table 1 The particle size ranges (Dp) and human organ invaded by atmospheric particles corresponding to the level of the sampler

Level	Dp (μm)	Human organ
0	>9.0	nasal cavity
1	5.8-9.0	nasal cavity
2	4.7-5.8	throat
3	3.3-4.7	bronchi
4	2.1-3.3	bronchi
5	1.1-2.1	bronchi
6	0.7-1.1	alveoli
7	0.4-0.7	alveoli

8	<0.4	alveoli

2.2 Elemental analysis

All the collected particle samples were dried for 48h and half of each filter paper were put into a polytetrafluoroethylene (PTFE) digestion vial where 65% HNO_3 (3.75 mL), 40% H_2O_2 (1.25 mL) and 30% HF (0.20 mL) were added successively. Then the solutions were heated by the oven (Yamato), with the temperature and duration of 185℃and 8h, respectively. After the heating process, the digested particles samples were dilutedwith distilled water constant volume to 15 mL. Finally, 6 mL of the sample solution was taken out and the concentrations of MEs were measured by ICP-OES (iCAP™ 7000 Series, Thermo Scientific™, MA, USA) and ICP-MS (Agilent Technologies, Tokyo, Japan), simultaneously. In addition, internal standards (^{89}Y, ^{193}Ir, ^{115}In and ^{103}Rh) were added online during MEs analysis (Pan and Wang, 2015).

2.3 Quality assurance (QA) and quality control (QC)

The pre-treatment and analytical procedure of samples followed a strict QA/QC process. The replicate field blanks and filter samples were handled identically to assess the error during both sampling and data processing (Pekney and Davidson, 2005). In order to assess the validity of data and select a group of reliable data obtained by two instruments, the limits of detection (LODs) were calculated as three times the standard deviation (SD) for the blank samples. All results are listed in Table 2. which also shows the calculated mean and SD of ME concentration in the filter samples.For the two analytic techniques of ICP-OES and ICP-MS, the average concentrations and SD of MEs in the size-resolved particles were calculated separately then summarized in the supplement table and to prevent misuse of the data below the LODs of these instruments, they were listed as <b.d.l. and omitted in the data processing. The average concentrations of blanks samples were well below that of filter samples and MEs' concentrations in the filter samples were above LODs so that blank samples did not exert an important influence on the observed concentrations. However, the average concentrations of As, Se and Pb of filter samples were below that of blank samples and the concentrations of Mg, Al and Ca in the field blanks were below the LODs of

instrument, which were analyzed by ICP-OES. In addition, Fe and Zn, abundant in the environment, could be measured more accurately by ICP-OES (Cruz et al., 2015). So the concentrations of Na, K, Fe and Zn used the data of ICP-OES, while that of other MEs chose from ICP-MS.

Additionally, reference materials of fly ash (GBW08401) and soil (GBW07401) were acid digested and measured in parallel with the filters samples to measure the recoveries (Pan et al., 2015). The recoveries of MEs are within the target recoveries (100 ±15%), with the exception of Se. Thus, this study only presents 23 MEs (As, Fe, Pb, Cd, Ni, Cu, Zn, Cr, Ti, Al, K, Na, Mn, V, Ba, Tl, Be, Co, Sr, Mo, Ag, Sn, U).

Table 2. Field blanks and limit of detection of the MEs subject to microwave digestion with $HNO_3/H_2O_2/HF$.

Elements	ICP-OES		ICP-MS	
	Air ($ng \cdot m^{-3}$) [a]	Limit of detection ($ng \cdot m^{-3}$) [c]	Air ($ng \cdot m^{-3}$) [b]	Limit of detection ($ng \cdot m^{-3}$) [d]
Na	85.04	56.32		
Mg	-1.40	1.95		
Al	-0.87	3.36	0.815	0.919
K	16.53	23.88		
Ca	-2.85	1.19		
V	-0.20	6.24	0.003	0.008
Cr	0.38	8.73	0.027	0.100
Mn	0.07	1.60	0.012	0.013
Fe	0.75	4.27	0.175	0.299
Ni	-2.87	10.46	0.010	0.008
Cu	-1.94	2.69	0.048	0.082
Zn	1.04	3.18	0.131	0.142
As	83.51	84.05	0.004	0.006
Se	60.44	76.98	0.005	0.010
Mo			0.015	0.034
Cd	1.47	4.61	0.002	0.001
Ba	0.09	0.21	0.009	0.032
Pb	38.11	66.65	0.044	0.172
Ti	-1.90	3.75	0.037	0.144
Tl	-58.57	63.69	0.001	0.001
Be	-0.63	0.71	0.000	0.000
Co			0.002	0.004
Sr			0.049	0.011
Ag			0.031	0.019

Sn	0.039	0.109
Sb	0.023	0.070
U	0.001	0.002

Note: [a] and [b]: Field blanks in air were respectively calculated to be equal to mean values of element mass concentrations in six filter blanks used by the ICP-OES and ICP-MS;

[c] and [d]: Limit of detection (LOD) corresponding to three times the standard deviation of the six blank signals obtained by using the ICP-OES and ICP-MS respectively.

2.4 Data analysis

2.4.1 Enrichment factor

To evaluate the contamination level of metal elements, the crustal enrichment factors (EFs) were calculated as follows (Luo et al., 2015):

$$EF = \frac{(C_i/C_R)sample}{(C_i/C_R)background} \quad (1)$$

where, C_i and C_R are the concentrations of selected MEs and reference element in sample and background crust (Cheng et al., 2014), respectively. Aluminum served as the reference element in this study. This method facilitates the determination of the source contribution of MEs originated from natural and anthropogenic emissions (Wang et al., 2018). In general, EF$\leqslant$1 indicates that MEs are mainly from natural sources such as road dust, while EF$>$1 is deemed to be from anthropogenic sources. The larger the value of EF, the higher the degree of enrichment of MEs.

2.4.2 The geo-accumulation index

The geo-accumulation index (I_{geo}) is introduced to draw a comparison between the background levels and concentrations of MEs in particles to analysis local pollution levels of MEs (Censi et al., 2017; Li et al., 2015), calculated by Eq. (2) (Müller, 1969):

$$I_{geo} = log_2 \frac{(C_i)sample}{1.5\times(C_i)background} \quad (2)$$

where, the meanings of C_i are equal to that of EF and same data are used to calculate it. The factor 1.5 is applied as the background matrix correction value. The pollution levels of MEs at sampling site are divided into seven categories according to the values of I_{geo}: uncontaminated ($I_{geo}\leqslant 0$), slightly contaminated ($0< I_{geo}\leqslant 1$), moderately contaminated ($1<I_{geo}\leqslant 2$), moderately to strongly contaminated ($2< I_{geo}\leqslant 3$), strongly contaminated

168 ($3<I_{geo}\leqslant 4$), strongly to severely contaminated ($4< I_{geo}\leqslant 5$), and severely contaminated
169 ($I_{geo}> 5$) (Wei et al., 2015).

170 2.4.3 The potential ecological risk index

171 This study used the potential ecological risk index proposed by Hakanson (1980)
172 to evaluate the environmental influence of heavy metal elements in particles. The
173 method builds up a bond between the environmental ecological effect and toxicological
174 characteristics of heavy metals, comprehensively assessing the potential risk of heavy
175 metals in environment. The potential ecological risk index of a single element (E^i_r) and
176 comprehensive potential ecological risk index (RI) can be calculated by using the
177 following equations:

178 $$C_f^i = (C_i)sample/(C_i)background \quad (3)$$

179 $$E_r^i = T_r^i \times C_f^i \quad (4)$$

180 $$RI = \sum E_r^i \quad (5)$$

181 where, the meanings of C_i are equal to that of EF and I_{geo}, C_f^i is the contamination factor
182 of the metal i and T_r^i is the toxic-response factor of the metal i, which is determined
183 for Ti=Mn=Zn=1, V=Cr=2, Cu=Ni=Co=Pb=5, Tl=As=10 and Cd=30 according to
184 previous studies (Douay et al., 2013; Egbueri, 2020; Liu et al., 2018). Due to little
185 toxicological effects for mineral elements and absence of T_r^i of some elements, the
186 potential ecological risks of only 12 elements (Zn, Co, V, Cr, Mn, Ti, Ni, Cu, As, Cd,
187 Tl and Pb) were analyzed in this study. On the basis of its severity, the ecological risks
188 were divided into five levels: slight risk ($E^i_r<40$); moderate risk ($40<E^i_r<80$); strong
189 risk ($80<E^i_r<160$); very strong risk ($160<E^i_r<320$); extremely strong risk ($E^i_r>320$).
190 Similarly, the scopes of RI were ~150, 150~300, 300~600 and 600~ for low ecological
191 risk, moderate ecological risk, high ecological risk and very high ecological risk (Gujre
192 et al., 2021; Williams and Antoine, 2020).

193 ## 3. Results and discussion

194 ### 3.1 Particle mass concentration

195 The air quality is classified into four levels: clear ($PM_{2.1}\leqslant 50$ μg·m^{-3}), slight

pollution ($50<PM_{2.1}\leqslant100$ μg·m^{-3}), moderate pollution ($100<PM_{2.1}\leqslant150$ μg·m^{-3}), and severe pollution ($PM_{2.1}>150$ μg·m^{-3}). The average mass concentrations of $PM_{2.1}$ in Beijing were 24.16 μg·m^{-3}, 94.34 μg·m^{-3}, 127.88 μg·m^{-3}, 200.89 μg·m^{-3} in four levels, respectively. Fig. 2 showed that the size distributions of particle mass concentrations were all bimodal in four levels. The first peak was in the fine fraction (0.4~2.1 μm) and the second peak occurred in the coarse fraction (3.3~5.8 μm). Atmospheric particles in the coarse fraction were accumulated in all aerosol conditions including clear and slight pollution, accounting for 30.98% and 25.36% of total mass concentration, respectively. However, the atmospheric particles in fine fraction had relatively larger contributions under moderate pollution and severe pollution (22.08% and 20.55%) compared to that in coarse fraction (19.46% and 18.01%). These observations revealed that as the pollution level intensified, the concentrations of fine particles, especially at the size range of 0.4-2.1 μm, increased, which was the main cause of the deterioration of air quality in Beijing. In comparison, the average mass concentration of fine particles in 2013 prior to air quality legislation ranged from 148.69 to 180.00 μg·m^{-3}, which was higher than that of our result (111.80 μg·m^{-3}). Moreover the size distribution of particle mass concentrations was centered at $Dp\leqslant1.0$ μm, accounting for approximately 63.50~72.70% of total concentration (Wang et al., 2014; Zhu et al., 2016). It is showed that the main constituents of atmospheric particles were fine particles in Beijing in 2013. In addition, Shao et al. (2018) also observed the downward trend of annual fine particles concentration from 2013 to 2016 in Beijing. These phenomena revealed the important effect of the *Chinese Air Pollution Prevention Action Plan* released in 2013, alleviating the atmospheric pollution situation in Beijing obviously and manifesting the size distribution as the coarse fraction was as important as the fine fraction in particles in Beijing.

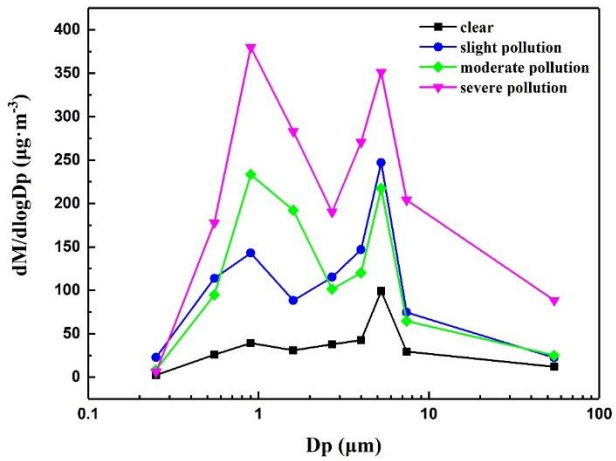

Fig. 2. Size distributions of particle mass concentration in different air quality levels

3.2 Element concentration and size distribution

3.2.1 Elemental concentrations in size-resolved particles

Atmospheric particles with high loading of MEs will cause adverse effects on the environment and human health. Based on the cut points of the sampler, the atmospheric particles were further divided into fine mode (<2.1 μm), coarse mode (2.1-9.0 μm), and large mode (>9.0 μm). As shown in Fig. 3, the atmospheric MEs generally accumulated more in the fine and coarse mode particles than that in large mode particles, with the average concentrations of 19.22, 19.31, and 5.36 $\mu g \cdot m^{-3}$, respectively, which was consisted with previous research (Pan et al., 2013; Zhang et al., 2019). This suggests that smaller particles with higher specific surface areas have more active sites around the surfaces and stronger adsorption in the fine and coarse mode, compared with large mode particles.

MEs can be divided into mineral elements (Na, Fe, Al, K) and heavy metal elements (other 19 elements). The average concentrations of mineral elements were 2~5 orders of magnitude higher than heavy metals in samples. The contents of Na were all the highest among the mineral elements in three mode particles, followed by Fe, Al, K. Moreover, the mineral elements tended to be enriched in the particles with size range lower than 9.0 μm. For heavy metals, Zn was the most abundant element, followed by Ti, Mn, Cr, Ba, and Pb, while other heavy metals accounted for a relatively small proportion by mass in particles.

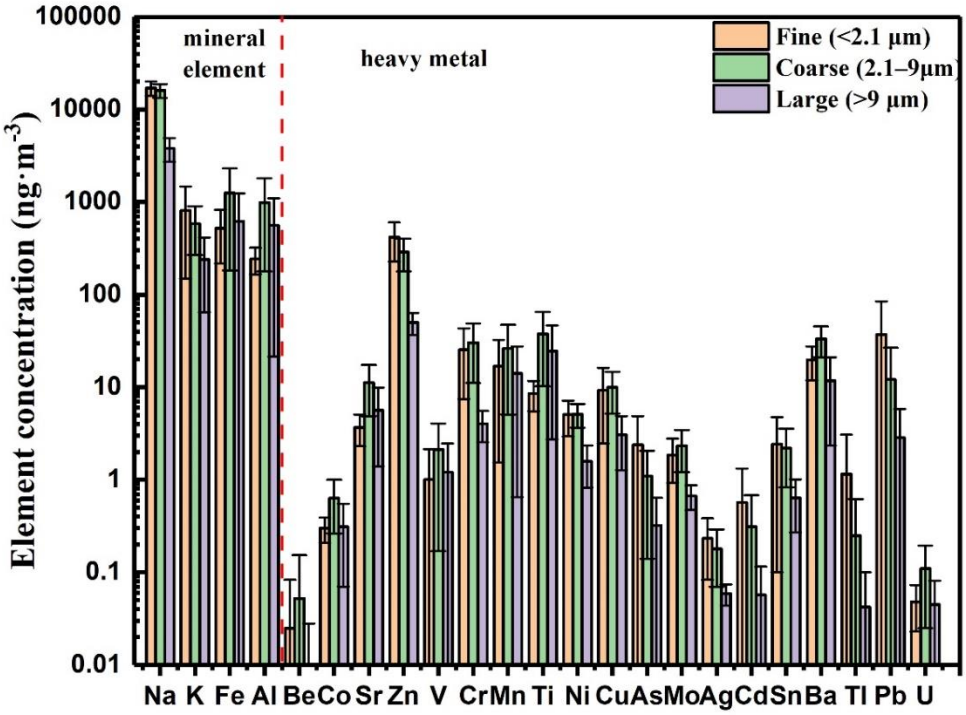

Fig. 3. Mass concentrations of metal elements in size-resolved particles

3.2.2 Size distribution

According to the similarities of the size distributions, 23 MEs were clarified into three groups.

The first group included Fe, Co, Sr, Al, Ti, Ba, and U, which were abundant in coarse mode with the majority of the mass centered at 4.7 μm and 5.8 μm (Fig. 4(a)), indicating that they mainly originated from natural sources, e.g., coarse particles produced by mechanical processes (Kandler et al., 2009). These elements in the coarse fraction (3.3~5.8 μm) accounted for 52.31% (U)~71.37% (Ti), in contract, these elements in large model particles were ultra-low with the percentage of only 5.01% of the total concentration. Considering the location of the sampling site, it can be inferred that the main source of these elements was the road dust caused by soil suspension and accumulated wind-blown dust, not anthropogenic emission (Gao et al., 2014; Ji et al., 2016). In addition, the size distributions of Co, Sr, Al, Ti, Ba, U varied from unimodal to bimodal distribution from clear to severe pollution (Supplement figure), which is most likely caused by the vehicle exhaust emission and regional transmission in Beijing

(Pan et al., 2013; Tong et al., 2020).

The second group consisted of Zn, As, Cd, Tl, and Pb, and these elements only had a peak in the fine mode (Fig. 4(b)), which suggested the effect of anthropogenic sources. Among these five elements, As, Cd, Tl, and Pb had a peak in the fine fraction (0.4~2.1 μm), and their percentages ranged from 53.22% (Cd) to 75.79% (Tl) of the total concentrations. In addition, these four elements all turned into bimodal distribution under moderate and severe pollution and showed an additional minor peak at 4.7~5.8 μm (Supplement figure). Linak et al. (2000) showed that As, Pb and Cd from incineration chambers had similar bimodal particle size distribution. Hence, these MEs were mainly caused by coal combustion during the heating period in winter. As for Zn, its concentration wasconcentrated in a wide particle size range from 0.7 to 5.8 μm, and the contribution concentration at 0.7~2.1 μm occupied about 52.54% of the total concentration, mainly causing by vehicle emissions and road dust (Chen et al., 2010). Moreover, the average concentration of Zn in our clear pollution level (0.41 $\mu g \cdot m^{-3}$) was higher than that of slight pollution (0.31 $\mu g \cdot m^{-3}$), and the average concentration in moderate pollution (0.59 $\mu g \cdot m^{-3}$) was similar to that of severe pollution (0.56 $\mu g \cdot m^{-3}$), indicating that the content of Zn had no positive correlation with air pollution level and the effect of natural sources was as significant as that of anthropogenic activities.

The third group including Na, K, Be, V, Cr, Mn, Ni, Cu, Mo, Ag and Sn, presented a bimodal distribution, with the first peak at fine mode (0.4~2.1 μm) and the second peak at coarse mode (3.3~5.8 μm) (Fig. 4(c)), in line with multiple sources, i.e., natural and anthropogenic emissions. These elements in the fine mode accounted for 19.29% (Be) to 41.21% (K) of the total concentration and 44.44% (K) to 61.98% (V) in coarse mode. The elemental concentrations were all relatively high in two fractions, but more centralized in the coarse mode, indicating that these elements mainly caused by road dust. In addition, the size distributions of V, Cr and Mn were unimodal structure with a peak at coarse mode under clear and slight pollution (Supplement figure). Be and Ni showed various distribution forms under four levels, but more accumulated in the coarse mode particles, particularly in moderate and severe pollution, manifesting that these elements were rarely affected by the anthropogenic sources. As the pollution

levels aggravated, the loading concentration of K within submicron particles smaller than 0.7 μm was increased, which may be attributable to biomass burning (Li et al., 2014; Silva et al., 1999).

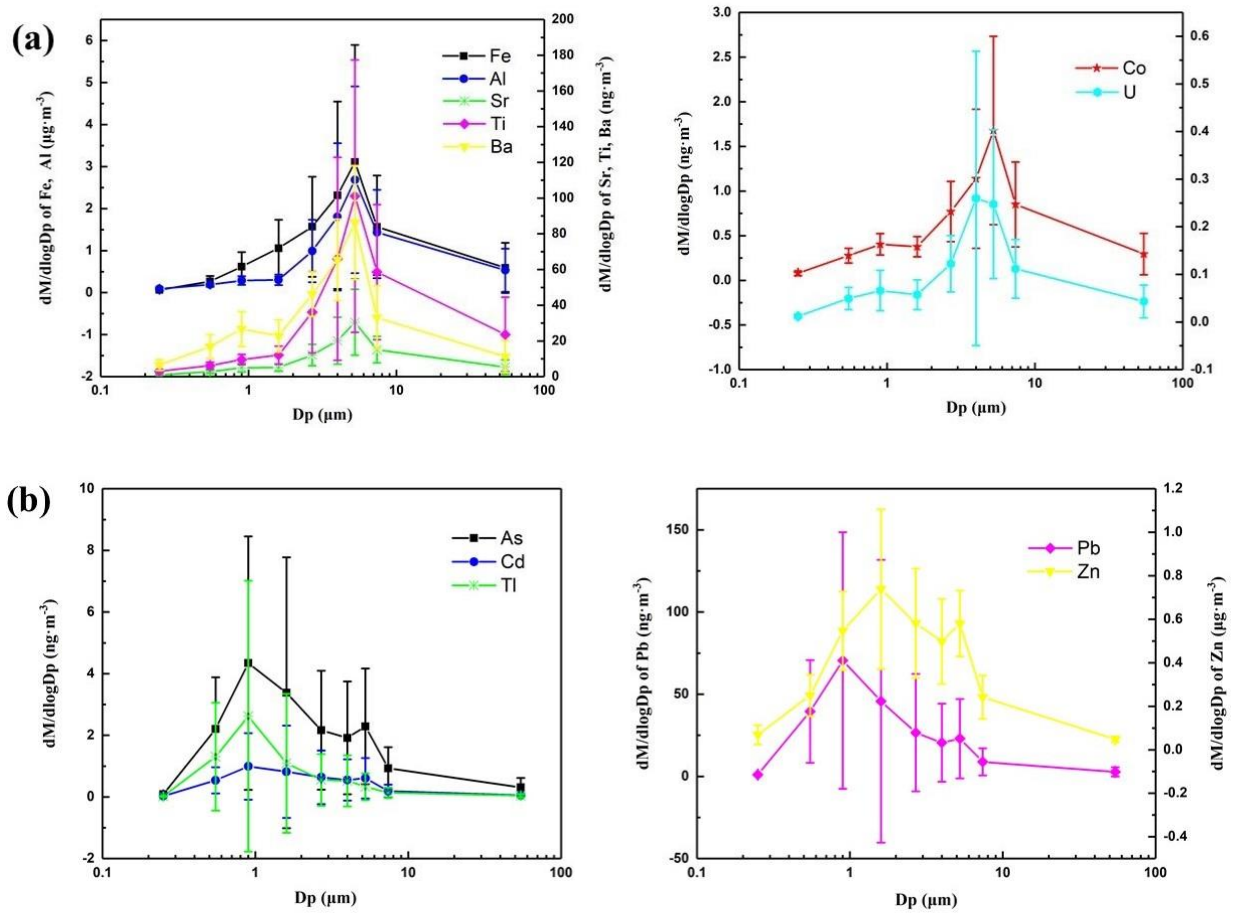

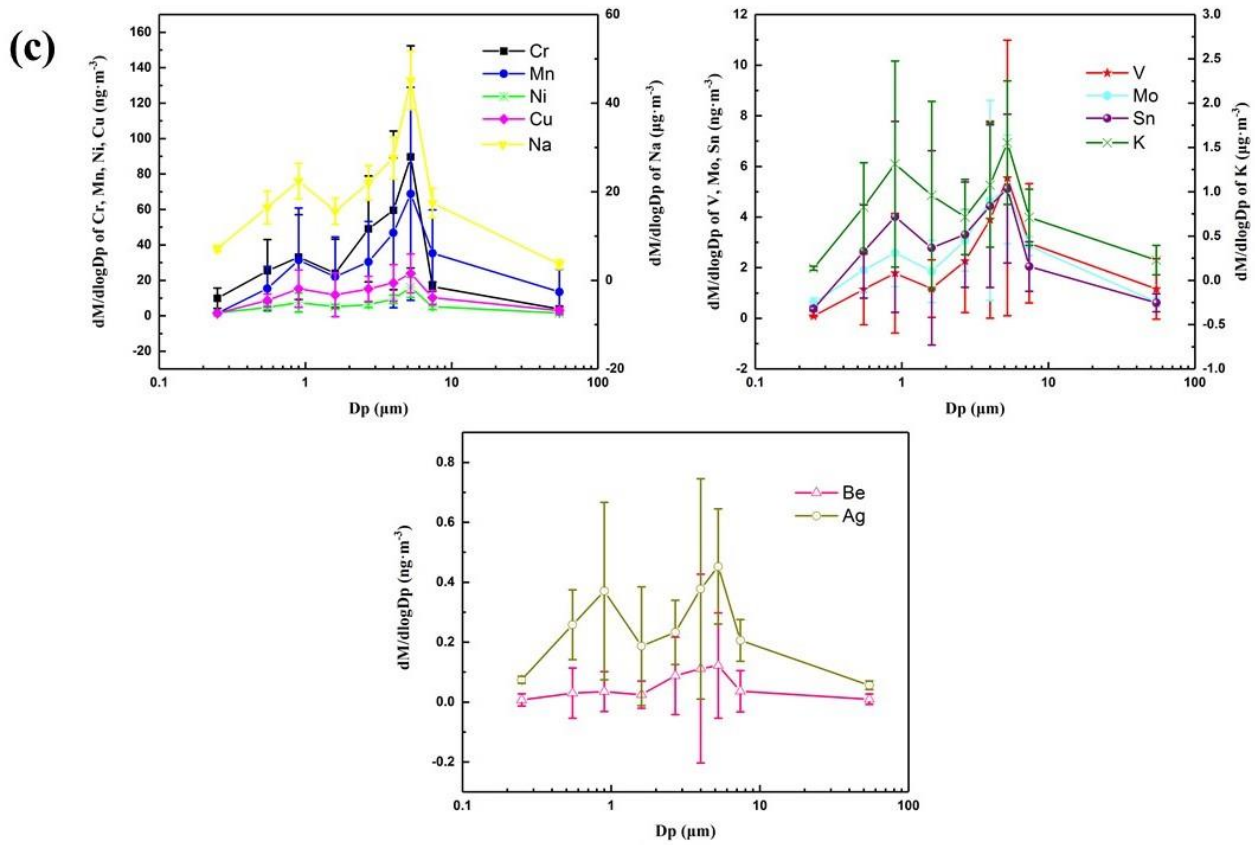

Fig. 4. The size distributions of selected 23 metal elements in particles during the Beijing winter (unimodal in coarse mode (a), unimodal in fine mode (b), and bimodal (c)). The data point is the average concentration of metal elements during eight sampling periods and the error bar is SD.

3.3 Source determined by enrichment factor

Enrichment factor (EF) was employed to evaluate the contamination level and differentiate the source contribution of MEs originated from natural and anthropogenic emissions. Fig. 5 showed the average enrichment of MEs in different mode particles. For TSP, the EF value of Ti was less than 1, which was from natural sources. Other MEs in TSP could be divided into three groups according to their EFs values. The values of EFs for K, Fe, Be, Co, Sr, V, Mn, Ba and U were relatively low（＜10), particularly in the large mode particles, suggesting that these elements, slight degree of enrichment, mainly originated from re-suspended soil (Polidori et al., 2009). Cr, Ni, Cu, As, Sn, Pb showed the intermediately enriched group with EFs between 10 and 100. And other six elements (Na, Zn, Mo, Ag, Cd, and Tl) were dominated by anthropogenic sources (vehicle exhaust emissions and combustion process) (Huang et al., 1994), and the

highly enriched group with the EFs higher than 100. Moreover, Zn, Mo and Cd had the highest EFs in each size fraction (EF exceed or was approximately equal to 100), indicating that the worst-affected elements were Zn, Mo and Cd of selected 23 MEs by anthropogenic sources. The elements of Cr, Ag, Tl, Sn and Pb also became high enrichment degree in fine mode particles, moreover, the EF of Zn even exceeded 1000. So these heavy metals were mainly influenced by anthropogenic emissions. In addition, Na was a mineral element, while its EF values in large, coarse and fine particles were relatively high (36.49, 86.39 and 374.61). Oetari et al. (2019) and Meij and te Winkel (2007) have confirmed that the content of Na in atmospheric particles had strong relationship with coal combustion. Hence, in this study, the high enrichment of Na was likely derived from combustion sources during the heating period in winter combined with the sampling site, locating on the rural-urban fringe zone. The comparison of the EFs for each element among 3 different size fraction showed that the enrichment levels of elements increased as particle size decreased, which was consisted with previous researches (Pan et al., 2013; Pancras et al., 2013), revealing the significant environment effect of fine particles.

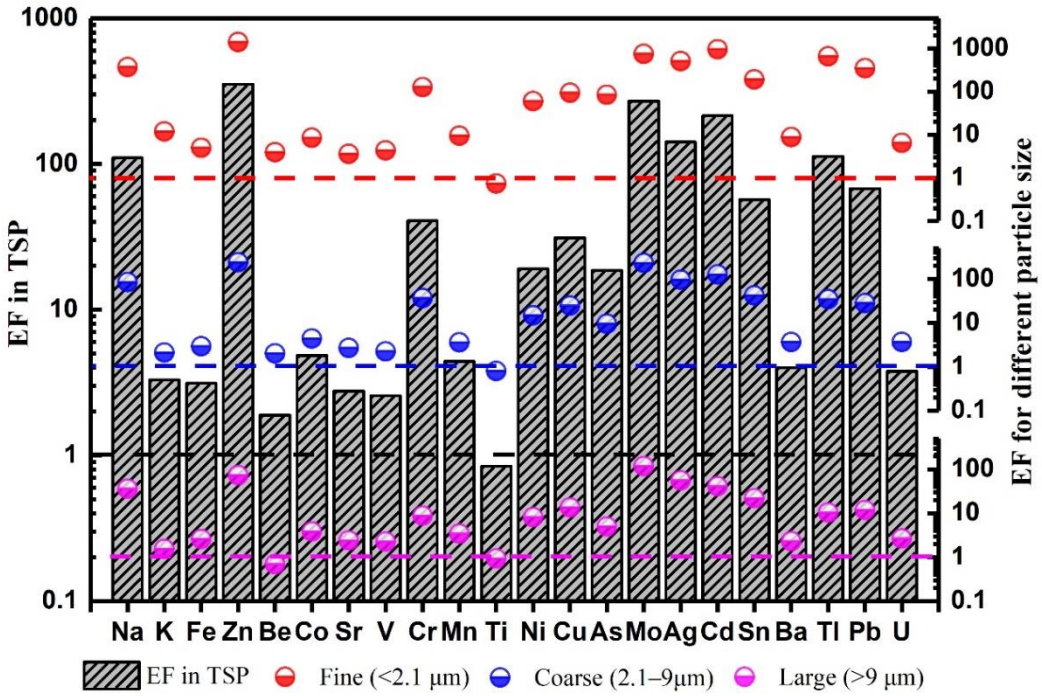

Fig. 5. Enrichment factors (EFs) of metal elements in TSP, fine mode, coarse mode, and large mode particles in Beijing. EF=1 in TSP and different size-resolved particles was marked by the dash line, colored by corresponding color.

3.4 Environmental risk assessment

To evaluate the overall environmental pollution degree and ecological risk in Beijing, the concentrations of MEs in TSP, obtained by adding the average concentrations of 9 size ranges, were used to calculate I_{geo} and the potential ecological risk index. As shown in Fig. 6, the I_{geo} values of K, Fe, Be, Co, Sr, Al, V, Mn, Ti, Ba and U were less than 0, indicating that these MEs can not cause environment contamination. Moreover, these elements of $I_{geo}<0$ displayed no or low degree of enrichment combined with the values of EFs. It was confirmed that the effect of MEs originated from anthropogenic emissions was more significant than that from natural sources on the environment. The average I_{geo} values of Ni and As were smaller than 1, and that of Na, Cr, Cu, Ag, Cd, Sn, Tl and Pb were between 1 and 4, which revealed slight contamination by Ni and As, and moderate to strong contamination by Na, Cr, Cu, Ag, Cd, Sn, Tl and Pb. However, 25.00% of the sampling periods belonged to strongly to severely contaminated categories for Na, Ag and Cd ($4 \leqslant I_{geo} \leqslant 5$). The I_{geo} values of Zn and Mo were the highest of all MEs with main ranges of I_{geo} (Zn)>5 and $4 \leqslant I_{geo}$ (Mo)$\leqslant 5$; thus these two elements could cause serious pollution for the environment.

Fig. 7 indicated the potential ecological risk index of 12 heavy metals, and the comprehensive potential ecological risk index (RI) was calculated during the sampling period. The values of RI ranged from 363.97 to 2054.02 with a mean value of 926.87, demonstrating that the atmospheric particles showed the high potential ecological risk during winter time in Beijing. To be specific, Cd, Tl, Zn, and Pb were the most important pollution elements for the environment, with the E^i_r values of 759.97, 105.91, 67.95, and 41.20, respectively. Hence, it is significant to identify the sources of these four elements and decrease their emission amounts, especially Cd. The comparatively higher ecological risks posed by Cd and Cu in the road dust of industrial areas have

been attributed to smelting and ironworks, and electronic wastes from factories, but not existed in Beijing (Shahab et al., 2020). Therefore, we can infer that atmospheric particles contained Cd may come from regional transmissions of peripheral steel smelting plants, be deposited onto road, thereby exerting adverse potential ecological risk on environment.

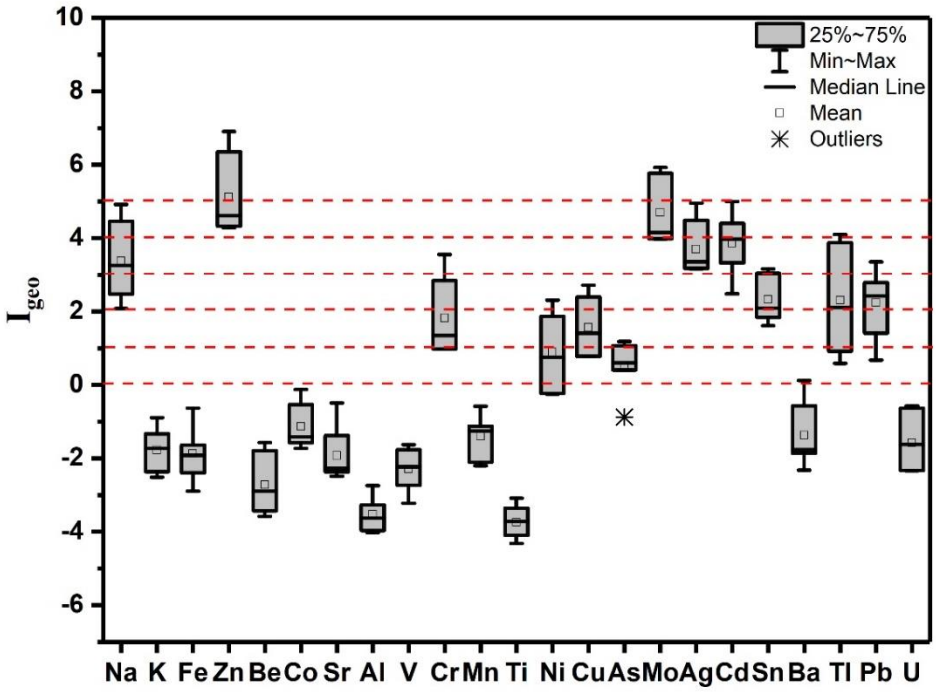

Fig. 6. The geo-accumulation index (I_{geo}) of elements from January to March 2016 in Beijing

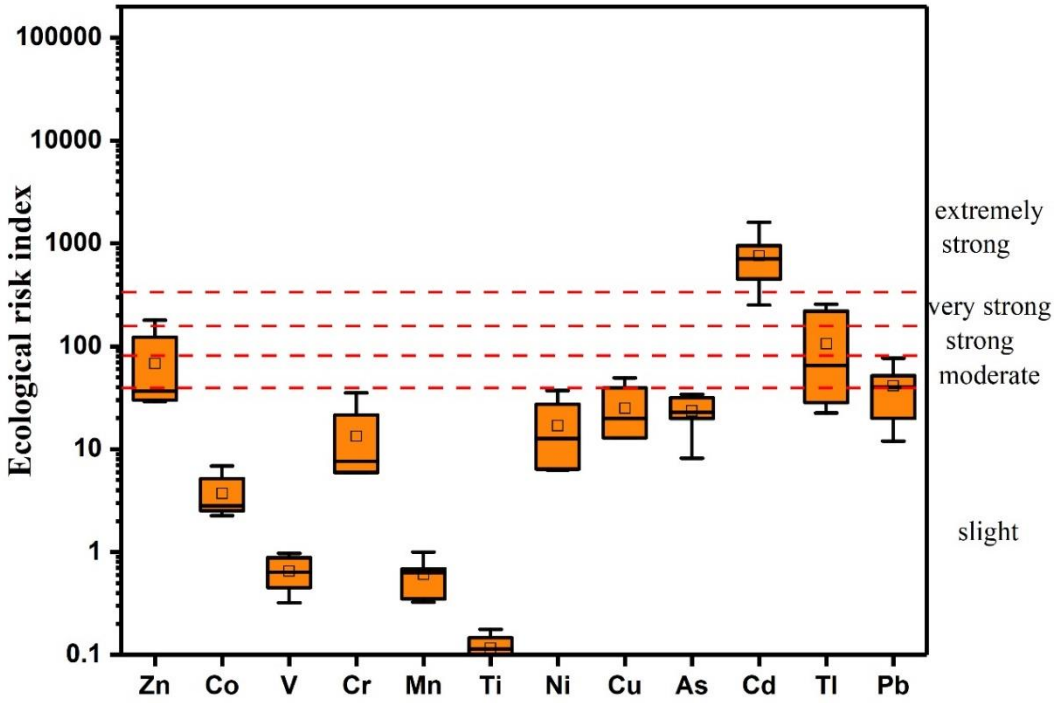

Fig. 7. The potential ecological risk of heavy metals in atmospheric particles

The ecological risks of 12 heavy metals were divided into five levels according to the values of E^i_r as described above and the corresponding level limits were marked by red dash line in the figure.

4. Conclusions

The size-resolved atmospheric particulate samples in Beijing were collected to analyze the size distributions of particle mass concentrations and selected 23 MEs during January to March 2016. Combined with the EF analysis and other model parameters, the intensive data analysis campaigns investigated the source of MEs in particles and evaluated their environmental risks. The results lead to the following conclusions.

(1). The size distributions of particle mass concentrations all were bimodal in four air quality levels, i.e., the first at fine fraction (0.4~2.1 μm) and the second at coarse fraction (3.3~5.8 μm). The atmospheric particles were accumulated easily in coarse fraction in clear and slight pollution. But under moderate and severe pollution, the proportion of particles in the fine fraction increased and in the coarse mode decreased, showing the significant emissions of fine

particles in Beijing, in accord with the comparison of the EFs among 3 different size fractions.

(2). According to the similarities of the size distributions, 23 MEs are divided into three groups: (a) elements (Fe, Co, Sr, Al, Ti, Ba, U) showing the unimodal distribution, which were abundant in coarse mode; (b) elements (Zn, As, Cd, Tl, Pb) showing unimodal structure with a peak in fine mode particles; (c) elements (Na, K, Be, V, Cr, Mn, Ni, Cu, Mo, Ag, Sn) with a bimodal distribution throughout the size range (centered at approximately 0.55~1.60 μm and 4.00~7.40 μm). The size distributions of MEs in four air quality levels varied greatly. For the MEs of unimodal distribution, most elements maintained their original size distributions under clear and slight pollution, while in the case of severe pollution, showing the bimodal distribution, except for Fe and Zn. These findings suggest that the composition of coarse particles is as important as that of fine particles to alleviate heavy metal pollution in the modern urban atmosphere.

(3). The source emission and environmental risk varied with the elemental composition of atmospheric particles and were identified by the factor analysis applied on the elemental data combined with the size distributions. Na, Zn, Mo, Ag, Cd, and Tl showed high enrichment degrees and moderate to severe contamination on the environment, signifying influences from regional transmissions or anthropogenic emissions, e.g., vehicle exhaust emissions and coal combustion. Other elements may originate from multiple sources, i.e., anthropogenic emissions and road dust, except for Ti. In addition, Beijing's atmospheric particles showed the high potential ecological risk in winter according to the values of RI. To be specific, Cd, Tl, Zn, and Pb were the most important pollution elements for the environment, with the E^i_r values of 759.97, 105.91, 67.95, and 41.20, respectively. Hence, the pollution of metal elements should cause concern for people, especially Cd.

Acknowledgments

Funding: This work was supported by the National Research Program for Key Issues in Air Pollution Control (No.DQGG0304-05) and the Fundamental Research Funds for Central Public Welfare Scientific Research Institute of China (No.2016YSKY-025). The European Commission Marie Skłodowska Curie Career Integration Grant supported time and resource for SJU (PCIG-GA-2012-778 333143 'DISCOSAT').

References

Acosta, J.A., Faz, Á., Kalbitz, K., Jansen, B., Martínez-Martínez, S., 2011. Heavy metal concentrations in particle size fractions from street dust of Murcia (Spain) as the basis for risk assessment. J. Environ. Monit. 13, 3087–3096. https://doi.org/10.1039/c1em10364d

Allen, A.G., Nemitz, E., Shi, J.P., Harrison, R.M., Greenwood, J.C., 2001. Size distributions of trace metals in atmospheric aerosols in the United Kingdom. Atmos. Environ. 35, 4581–4591. https://doi.org/10.1016/S1352-2310(01)00190-X

Bilos, C., Colombo, J.C., Skorupka, C.N., Rodriguez Presa, M.J., 2001. Sources, distribution and variability of airborne trace metals in La Plata City area, Argentina. Environ. Pollut. 111, 149–158. https://doi.org/10.1016/S0269-7491(99)00328-0

Censi, P., Cibella, F., Falcone, E.E., Cuttitta, G., Saiano, F., Inguaggiato, C., Latteo, V., 2017. Rare earths and trace elements contents in leaves: A new indicator of the composition of atmospheric dust. Chemosphere 169, 342–350. https://doi.org/10.1016/j.chemosphere.2016.11.085

Chen, X., Xia, X., Zhao, Y., Zhang, P., 2010. Heavy metal concentrations in roadside soils and correlation with urban traffic in Beijing, China. J. Hazard. Mater. 181, 640–646. https://doi.org/10.1016/j.jhazmat.2010.05.060

Cheng, H., Li, K., Li, M., Yang, K., Liu, F., Cheng, X., 2014. Geochemical background and baseline value of chemical elements in urban soil in China. Earth Sci. Front. 21, 265–306. https://doi.org/10.13745/j.esf.2014.03.028

Cruz, S.M., Schmidt, L., Dalla Nora, F.M., Pedrotti, M.F., Bizzi, C.A., Barin, J.S., Flores, E.M.M., 2015. Microwave-induced combustion method for the determination of trace and ultratrace element impurities in graphite samples by ICP-OES and ICP-MS. Microchem. J. 123, 28–32. https://doi.org/10.1016/j.microc.2015.05.008

Douay, F., Pelfrêne, A., Planque, J., Fourrier, H., Richard, A., Roussel, H., Girondelot, B., 2013. Assessment of potential health risk for inhabitants living near a former lead smelter. Part 1: Metal concentrations in soils, agricultural crops, and homegrown vegetables. Environ. Monit. Assess. 185, 3665–3680. https://doi.org/10.1007/s10661-012-2818-3

Duan, J., Tan, J., Hao, J., Chai, F., 2014. Size distribution, characteristics and sources of heavy metals in haze episod in Beijing. J. Environ. Sci. (China) 26, 189–196. https://doi.org/10.1016/S1001-0742(13)60397-6

Egbueri, J.C., 2020. Groundwater quality assessment using pollution index of groundwater (PIG), ecological risk index (ERI) and hierarchical cluster analysis (HCA): A case study. Groundw. Sustain. Dev. 10, 100292. https://doi.org/10.1016/j.gsd.2019.100292

Eleftheriadis, K., Ochsenkuhn, K.M., Lymperopoulou, T., Karanasiou, A., Razos, P., Ochsenkuhn-Petropoulou, M., 2014. Influence of local and regional sources on the observed spatial and temporal variability of size resolved atmospheric aerosol mass concentrations and water-soluble species in the Athens metropolitan area. Atmos. Environ. 97, 252–261. https://doi.org/10.1016/j.atmosenv.2014.08.013

Gao, J., Tian, H., Cheng, K., Lu, L., Wang, Y., Wu, Y., Zhu, C., Liu, K., Zhou, J., Liu, X., Chen, J., Hao, J., 2014. Seasonal and spatial variation of trace elements in multi-size airborne particulate matters of Beijing, China: Mass concentration, enrichment characteristics, source apportionment, chemical speciation and bioavailability. Atmos. Environ. 99, 257–265. https://doi.org/10.1016/j.atmosenv.2014.08.081

Gao, Y., Lee, S.C., Huang, Y., Chow, J.C., Watson, J.G., 2016. Chemical characterization and source apportionment of size-resolved particles in Hong Kong sub-urban area. Atmos. Res. 170, 112–122. https://doi.org/10.1016/j.atmosres.2015.11.015

Gregory, K., Webster, C., Durk, S., 1996. Estimates of damage to forests in Europe due to emissions of acidifying pollutants. Energy Policy 24, 655–664. https://doi.org/10.1016/0301-4215(96)00055-9

Gujre, N., Mitra, S., Soni, A., Agnihotri, R., Rangan, L., Rene, E.R., Sharma, M.P., 2021. Speciation, contamination, ecological and human health risks assessment of heavy metals in soils dumped with municipal solid wastes. Chemosphere 262, 128013. https://doi.org/10.1016/j.chemosphere.2020.128013

Hakanson, L., 1980. An ecological risk index for aquatic pollution control.a sedimentological approach. Water Res. 14, 975–1001. https://doi.org/10.1016/0043-1354(80)90143-8

Hao, J., Ge, Y., He, S.Y., Lu, N., Wang, Q.G., 2018. Size distribution characteristics of metal elements in air particulate matter during autumn in Nanjing. Zhongguo Huanjing Kexue/China Environ. Sci. 38, 4409–4414. https://doi.org/10.19674/j.cnki.issn1000-6923.2018.0493

Huang, X., Olmez, I., Aras, N.K., Gordon, G.E., 1994. Emissions of trace elements from motor vehicles: Potential marker elements and source composition profile. Atmos. Environ. 28, 1385–1391. https://doi.org/10.1016/1352-2310(94)90201-1

Ji, H., Ding, H., Tang, L., Li, C., Gao, Y., Briki, M., 2016. Chemical composition and transportation characteristic of trace metals in suspended particulate matter collected upstream of a metropolitan drinking water source, Beijing. J. Geochemical Explor. 169, 123–136. https://doi.org/10.1016/j.gexplo.2016.07.018

Kampa, M., Castanas, E., 2008. Human health effects of air pollution. Environ. Pollut. https://doi.org/10.1016/j.envpol.2007.06.012

Kandler, K., Schütz, L., Deutscher, C., Ebert, M., Hofmann, H., Jäckel, S., Jaenicke, R., Knippertz, P., Lieke, K., Massling, A., Petzold, A., Schladitz, A., Weinzierl, B., Wiedensohler, A., Zorn, S., Weinbruch, S., 2009. Size distribution, mass concentration, chemical and mineralogical composition and derived optical parameters of the boundary layer aerosol at Tinfou, Morocco, during SAMUM 2006. Tellus, Ser. B Chem. Phys. Meteorol. 61, 32–50. https://doi.org/10.1111/j.1600-0889.2008.00385.x

Karaca, F., Anil, I., Alagha, O., 2009. Long-range potential source contributions of episodic aerosol events to PM10 profile of a megacity. Atmos. Environ. 43, 5713–5722. https://doi.org/10.1016/j.atmosenv.2009.08.005

Lee, P.K., Youm, S.J., Jo, H.Y., 2013. Heavy metal concentrations and contamination levels from Asian dust and identification of sources: A case-study. Chemosphere 91, 1018–1025. https://doi.org/10.1016/j.chemosphere.2013.01.074

Li, H., Shi, A., Zhang, X., 2015. Particle size distribution and characteristics of heavy metals in road-deposited sediments from Beijing Olympic Park. J. Environ. Sci. (China) 32, 228–237. https://doi.org/10.1016/j.jes.2014.11.014

Li, X., Wang, L., Wang, Yuesi, Wen, T., Yang, Y., Zhao, Y., Wang, Yingfeng, 2012. Chemical composition and size distribution of airborne particulate matters in Beijing during the 2008 Olympics. Atmos. Environ. 50, 278–286. https://doi.org/10.1016/j.atmosenv.2011.12.021

Li, Y., Schwandner, F.M., Sewell, H.J., Zivkovich, A., Tigges, M., Raja, S., Holcomb, S., Molenar, J. V., Sherman, L., Archuleta, C., Lee, T., Collett, J.L., 2014. Observations of ammonia, nitric acid, and fine particles in a rural gas production region. Atmos. Environ. 83, 80–89.

https://doi.org/10.1016/j.atmosenv.2013.10.007
Linak, W.P., Miller, C.A., Wendt, J.O.L., 2000. Comparison of particle size distributions and elemental partitioning from the combustion of pulverized coal and residual fuel oil. J. Air Waste Manag. Assoc. 50, 1532–1544. https://doi.org/10.1080/10473289.2000.10464171
Liu, B., Kang, S., Sun, J., Zhang, Y., Xu, R., Wang, Y., Liu, Y., Cong, Z., 2013. Wet precipitation chemistry at a high-altitude site (3,326 m a.s.l.) in the southeastern Tibetan Plateau. Environ. Sci. Pollut. Res. 20, 5013–5027. https://doi.org/10.1007/s11356-012-1379-x
Liu, Y., Wang, Q., Zhuang, W., Yuan, Yanli, Yuan, Yani, Jiao, K., Wang, M., Chen, Q., 2018. Calculation of Thallium's toxicity coefficient in the evaluation of potential ecological risk index: A case study. Chemosphere 194, 562–569. https://doi.org/10.1016/j.chemosphere.2017.12.002
Luo, X.S., Xue, Y., Wang, Y.L., Cang, L., Xu, B., Ding, J., 2015. Source identification and apportionment of heavy metals in urban soil profiles. Chemosphere 127, 152–157. https://doi.org/10.1016/j.chemosphere.2015.01.048
Meij, R., te Winkel, H., 2007. The emissions of heavy metals and persistent organic pollutants from modern coal-fired power stations. Atmos. Environ. 41, 9262–9272. https://doi.org/10.1016/j.atmosenv.2007.04.042
Müller, G., 1969. Index of geoaccumulation in sediments of the Rhine River. Geol. J. 2, 108–118.
Oetari, P.S., Hadi, S.P., Huboyo, H.S., 2019. Trace elements in fine and coarse particles emitted from coal-fired power plants with different air pollution control systems. J. Environ. Manage. 250, 109497. https://doi.org/10.1016/j.jenvman.2019.109497
Pacyna, J.M., Pacyna, E.G., 2001. An assessment of global and regional emissions of trace metals to the atmosphere from anthropogenic sources worldwide. Environ. Rev. https://doi.org/10.1139/a01-012
Pan, Y., Tian, S., Li, X., Sun, Y., Li, Y., Wentworth, G.R., Wang, Y., 2015. Trace elements in particulate matter from metropolitan regions of Northern China: Sources, concentrations and size distributions. Sci. Total Environ. 537, 9–22. https://doi.org/10.1016/j.scitotenv.2015.07.060
Pan, Y., Wang, Y., Sun, Y., Tian, S., Cheng, M., 2013. Size-resolved aerosol trace elements at a rural mountainous site in Northern China: Importance of regional transport. Sci. Total Environ. 461–462, 761–771. https://doi.org/10.1016/j.scitotenv.2013.04.065
Pan, Y.P., Wang, Y.S., 2015. Atmospheric wet and dry deposition of trace elements at 10 sites in Northern China. Atmos. Chem. Phys. 15, 951–972. https://doi.org/10.5194/acp-15-951-2015
Pancras, J.P., Landis, M.S., Norris, G.A., Vedantham, R., Dvonch, J.T., 2013. Source apportionment of ambient fine particulate matter in Dearborn, Michigan, using hourly resolved PM chemical composition data. Sci. Total Environ. 448, 2–13. https://doi.org/10.1016/j.scitotenv.2012.11.083
Pekney, N.J., Davidson, C.I., 2005. Determination of trace elements in ambient aerosol samples. Anal. Chim. Acta 540, 269–277. https://doi.org/10.1016/j.aca.2005.03.065
Polidori, A., Cheung, K.L., Arhami, M., Delfino, R.J., Schauer, J.J., Sioutas, C., 2009. Relationships between size-fractionated indoor and outdoor trace elements at four retirement communities in southern California. Atmos. Chem. Phys. 9, 4521–4536. https://doi.org/10.5194/acp-9-4521-2009
Schwartz, J., Dockery, D.W., Neas, L.M., 1996. Is Daily Mortality Associated Specifically with Fine Particles? J. Air Waste Manag. Assoc. 46, 927–939. https://doi.org/10.1080/10473289.1996.10467528
Shahab, A., Zhang, H., Ullah, H., Rashid, A., Rad, S., Li, J., Xiao, H., 2020. Pollution characteristics and toxicity of potentially toxic elements in road dust of a tourist city, Guilin, China: Ecological and health risk assessment☆. Environ. Pollut. 266, 115419.

https://doi.org/10.1016/j.envpol.2020.115419
Shao, P., Tian, H., Sun, Y., Liu, H., Wu, B., Liu, S., Liu, X., Wu, Y., Liang, W., Wang, Y., Gao, J., Xue, Y., Bai, X., Liu, W., Lin, S., Hu, G., 2018. Characterizing remarkable changes of severe haze events and chemical compositions in multi-size airborne particles (PM1, PM2.5 and PM10) from January 2013 to 2016–2017 winter in Beijing, China. Atmos. Environ. 189, 133–144. https://doi.org/10.1016/j.atmosenv.2018.06.038
Silva, P.J., Liu, D.Y., Noble, C.A., Prather, K.A., 1999. Size and chemical characterization of individual particles resulting from biomass burning of local Southern California species. Environ. Sci. Technol. 33, 3068–3076. https://doi.org/10.1021/es980544p
Tan, J., Zhang, L., Zhou, X., Duan, J., Li, Y., Hu, J., He, K., 2017. Chemical characteristics and source apportionment of PM2.5 in Lanzhou, China. Sci. Total Environ. 601–602, 1743–1752. https://doi.org/10.1016/j.scitotenv.2017.06.050
Taner, S., Pekey, B., Pekey, H., 2013. Fine particulate matter in the indoor air of barbeque restaurants: Elemental compositions, sources and health risks. Sci. Total Environ. 454–455, 79–87. https://doi.org/10.1016/j.scitotenv.2013.03.018
Tian, H., Cheng, K., Wang, Y., Zhao, D., Lu, L., Jia, W., Hao, J., 2012. Temporal and spatial variation characteristics of atmospheric emissions of Cd, Cr, and Pb from coal in China. Atmos. Environ. 50, 157–163. https://doi.org/10.1016/j.atmosenv.2011.12.045
Tong, R., Liu, J., Wang, W., Fang, Y., 2020. Health effects of PM2.5 emissions from on-road vehicles during weekdays and weekends in Beijing, China. Atmos. Environ. 223, 117258. https://doi.org/10.1016/j.atmosenv.2019.117258
Wang, F., Chen, D.S., Cheng, S.Y., Li, J.B., Li, M.J., Ren, Z.H., 2010. Identification of regional atmospheric PM10 transport pathways using HYSPLIT, MM5-CMAQ and synoptic pressure pattern analysis. Environ. Model. Softw. 25, 927–934. https://doi.org/10.1016/j.envsoft.2010.02.004
Wang, J., Hu, Z., Chen, Y., Chen, Z., Xu, S., 2013. Contamination characteristics and possible sources of PM10 and PM2.5 in different functional areas of Shanghai, China. Atmos. Environ. 68, 221–229. https://doi.org/10.1016/j.atmosenv.2012.10.070
Wang, J., Zhang, X., Yang, Q., Zhang, K., Zheng, Y., Zhou, G., 2018. Pollution characteristics of atmospheric dustfall and heavy metals in a typical inland heavy industry city in China. J. Environ. Sci. (China) 71, 283–291. https://doi.org/10.1016/j.jes.2018.05.031
Wang, Y.S., Yao, L., Wang, L.L., Liu, Z.R., Ji, D.S., Tang, G.Q., Zhang, J.K., Sun, Y., Hu, B., Xin, J.Y., 2014. Mechanism for the formation of the January 2013 heavy haze pollution episode over central and eastern China. Sci. China Earth Sci. 57, 14–25. https://doi.org/10.1007/s11430-013-4773-4
Wei, T., Dong, Z., Kang, S., Zong, C., Rostami, M., Shao, Y., 2019. Atmospheric deposition and contamination of trace elements in snowpacks of mountain glaciers in the northeastern Tibetan Plateau. Sci. Total Environ. 689, 754–764. https://doi.org/10.1016/j.scitotenv.2019.06.455
Wei, X., Gao, B., Wang, P., Zhou, H., Lu, J., 2015. Pollution characteristics and health risk assessment of heavy metals in street dusts from different functional areas in Beijing, China. Ecotoxicol. Environ. Saf. 112, 186–192. https://doi.org/10.1016/j.ecoenv.2014.11.005
Williams, J.A., Antoine, J., 2020. Evaluation of the elemental pollution status of Jamaican surface sediments using enrichment factor, geoaccumulation index, ecological risk and potential ecological risk index. Mar. Pollut. Bull. 157, 111288. https://doi.org/10.1016/j.marpolbul.2020.111288
Woszczyk, M., Spychalski, W., Boluspaeva, L., 2018. Trace metal (Cd, Cu, Pb, Zn) fractionation in

urban-industrial soils of Ust-Kamenogorsk (Oskemen), Kazakhstan—implications for the assessment of environmental quality. Environ. Monit. Assess. 190, 362. https://doi.org/10.1007/s10661-018-6733-0

Yu, J.Z., Huang, X.F., 2008. Size distributions of elemental carbon in the atmosphere of a coastal urban area in South China: Characteristics, evolution processes, and implications for the mixing state. Atmos. Chem. Phys. 8, 5843–5853. https://doi.org/10.5194/acp-8-5843-2008

Zereini, F., Alt, F., Messerschmidt, J., Wiseman, C., Feldmann, I., Von Bohlen, A., Müller, J., Liebl, K., Püttmann, W., 2005. Concentration and distribution of heavy metals in urban airborne particulate matter in Frankfurt am Main, Germany. Environ. Sci. Technol. 39, 2983–2989. https://doi.org/10.1021/es040040t

Zhai, L., Sun, Z., Li, Z., Yin, X., Xiong, Y., Wu, J., Li, E., Kou, X., 2019. Dynamic effects of topography on dust particles in the Beijing region of China. Atmos. Environ. 213, 413–423. https://doi.org/10.1016/j.atmosenv.2019.06.029

Zhang, X., Zhang, K., Lv, W., Liu, B., Aikawa, M., Wang, J., 2019. Characteristics and risk assessments of heavy metals in fine and coarse particles in an industrial area of central China. Ecotoxicol. Environ. Saf. 179, 1–8. https://doi.org/10.1016/j.ecoenv.2019.04.024

Zhu, Q., Zhang, X., Dong, S., Gao, L., Liu, G., Zheng, M., 2016. Gas and particle size distributions of polychlorinated naphthalenes in the atmosphere of Beijing, China. Environ. Pollut. 212, 128–134. https://doi.org/10.1016/j.envpol.2016.01.065